An Application for Superelastic Material in a Passive Inertial Damage Sensor for Detection of Conditions Leading to the Accumulation of Hidden Structural Damage Caused by Transient Loading in Aircraft
The Conception

J. Hoffman* and R. Jeffers
University of Connecticut, Department of Mechanical Engineering
191 Auditorium Road, Storrs Connecticut 06269

Abstract

The unusual properties of shape memory alloy have long tempted the engineering profession with its apparent possibilities. In this paper an aspect of shape memory, augmented by the property of superelasticity, is considered for use in sensing the occurrence of mechanical disturbances having severity sufficient to cause major damage within airborne structure or electronic modules. Often this damage occurs internally, i.e. below structure surfaces and thus is essentially invisible to inspection techniques that are performed in normal maintenance operations. The concept of a sensor is presented, herein, that can act as a witness to the occurrence of conditions that can produce such structural damage. The sensor, being passive in nature, carries its message in the permanent deformation of internal structure that is to be inspected at convenient intervals, between aircraft flights or after occurrence of seemingly severe aerodynamic or mechanical disturbances are encountered, to indicate the maximum levels of acceleration that it has witnessed. On the basis of such information, timely maintenance measures can be made to prevent impending failures from taking place. The location of such a sensor would serve to locate particular structure or components that would be susceptible to damage from the sensed levels of acceleration. This serves to focus maintenance inspection processes and indicate immediate preventive measures to be taken through replacement of, certain likely damaged structure, before the damage can accumulate to threaten the safety of the aircraft. The sensor concept is described herein, along with its expected properties and performance. This paper presents: (1) The basis for a general need for such a sensor; (2) A description of the sensor mechanization; (3) Aspects of shape memory and superelasticity relevant to its conception and purpose; (4) Test data illustrating the properties of the material and how they may be used to prevent further accumulation of damage; (5) Feasibility considerations in support of the concept and (6) Conclusions and objectives for continuing work.

The Need for a Damage Condition Sensor

On November 12, 2001 American Airlines Flight 587 out of Laguardia Airport experienced control problems during its take-off and this A300 Airbus crashed onto the city streets of New York, in the Belle Harbor district of Queens county, with loss of all 260 people on board and 5 more fatalities on the ground [1]. A seemingly similar accident occurred off the California coast near Los Angeles, in January 2000 [2], when an Alaska Airlines MD-83 twinjet was lost with 83 people on board. It was judged by the National Transportation Safety Board that, for both cases, the basic cause of these accidents was a structural damage accumulation in the tail sections of the two different aircraft.

These examples are presented to discriminate between two distinct types of damage accumulation, one of which can be avoided through the use of a damage occurrence sensor, while the other is a consequence of probable structural design flaws and not so easily detected.

For the case of the American Airlines flight, a likely immediate cause is an encounter with

* This identifies the author to correspondence should be addressed

extreme turbulence, reported just before the accident, emanating from the wake of a prior airplane take-off. Since such incidents are common at busy airports, the resulting catastrophe is judged to be a case of damage accumulation, of the type where one too many such events, caused by externally induced stress, finally produced a disaster that might have been avoided by a sensor that had recorded prior events of this nature, alerting maintenance personnel to the possible existence of damaged structure.

For the Alaska Airlines accident, a failed jackscrew was found to have produced a stabilizer break-off from the MD-83's T-tail. Damaged jackscrews, subsequently found in other aircraft of this type, indicate a gradual failure process where damage accumulation is thought to be the basic cause for this tragedy. Here, however, it is thought to be the result of a design or an assembly process flaw, effecting all such aircraft of this type, for which a damage occurrence sensor, of the type perceived herein, would not help.

In both cases the damage was not visible to maintenance personnel as it was hidden in structure having no apparent surface defects. Such occurrences are not restricted to air- craft structure, but also may occur in power plants and other essential components. Dam-age accumulation within the structure of electronic packages, is a constant concern to de-signers, who are faced with effects of flight environment as well as those of transportation and handling. Thus, a means to establish the presence of such damage is of value.

The only defenses against internal damage accumulation are by: (1) Periodic maintenance involving the replacement of defective parts, for which the maintenance policies are governed by measured statistics of known failure modes; or (2) By effective diagnostics to locate and redesign the structure to eliminate overstressed conditions. These are expensive measures involving high costs of implementation and loss of service time for the aircraft. However, for a damage mechanism not produced by design problems but rather by unexpected external loading events such as severe turbulence, as in the case of the American Airlines incident, another solution is possible.

Damage Sensor Design Objectives

A mitigation of the effects of random externally induced damage accumulation can be achieved by use of an appropriately designed sensor that can serve as a witness to incidents of transient force level occurrences and their directions. This can be accomplished by a capability to detect and record loading events that exceed allowable design limits of specific structure, previously identified in design or in failure mode analyses. Generally such events may be sensed by strain gages or accelerometers located on or near aircraft structure or components thereof for which damage occurrence is considered likely. This, however, involves accompanying instrumentation that requires active data storage capability, along with the recurring services of an analyst to interpret the results. Such systems are likely to be expensive to obtain, and install. Furthermore, due to their contributions to part count, these protective systems may have lower mean-times-to-failure than the very structural components they are meant to protect. Thus, the cost of their maintenance must also be borne. A passive sensor, using shape memory material, having a combined ability to detect and remember load levels and their directions, requires no data record, beyond the measurable permanent deformations provided by the conceived sensor. This will offer a less expensive and more reliable alternative. Establishing the feasibility of a sensor concept with such capability is the objective of this paper.

Describing the Concept for a Passive Inertial Damage Sensor

The key words in the above title are:

(a) Passive – Meaning the device will <u>not</u> provide an output signal proportional to maximum acceleration but rather, it will bear witness to that value by a measurable length change to one of its members, i.e. a witness wire, the measurement to be performed after a specific number of flight hours, using equipment located in a maintenance area of an airport.

(b) Inertial Condition– Meaning the measured condition of maximum accelerations the device had experienced in flight, captured in the deformation of a witness wire, accomplished through inertial loading effects produced upon a wire that is supporting a calibrated mass.

The physical nature of the sensor is described schematically in Figure 1a. It is seen to be comprised of four elements: (1) A seismic mass suspended symmetrically in the body of the instrument, (2) Two wires linking each side of the seismic mass to the casing of instrument. The wires, labeled "α" and "β", are made of drawn shape memory alloy. Note that (α) is always the wire in which tension is first established by the externally applied acceleration forces; (3) One or two threaded tension adjustment nuts (TA) may be used to simultaneously apply preload to both wires. (4) A cylindrical case containing the above three elements is used to isolate them from the ambient environment. The mass, seen in Figure 1a, to be supported laterally by a lubricated porous bushing, serves as the inertial sensing element of the system, imposing load on shape memory wires in response to accelerations applied along the wire axes. Thus, under acceleration, wire α is subjected to increased tensile load over that of the preloaded condition. The resulting wire deformation on the loading plateau, shown in Figure 1b, is a one-way effect that permits a wire to grow in length but never to shorten. The growth is due to a directionally oriented formation of newly developed variants of martensite material, which are the products of an ongoing stress-induced phase transformation. Thus the loading plateau of Figure 1b is a product of such transformation of the superelastic* shape memory material, used as the witness wires in the sensor concept. This effect occurs at a constant temperature condition, the value of this temperature establishing the stress level at which the loading plateau forms. A loading plateau, such as that seen in Figure 1b, is known to be the result of an exothermic process wherein the latent heat of phase transformation is lost in space and the stacking alignments of martensite crystals, resulting from the transformation, add up to produce what appears to be an accumulation of strain growth without the benefit of a significant stress increase. As a result of this type of formation, the process of strain accumulation cannot be reversed by a reversal of the applied inertial load. This fact is exploited, in the sensor design, by use of two wires, of such superelastic material, which provide a capability to discriminate between, as well as sense, the effects of positively and negatively directed acceleration inputs upon wire deformations.

It is noted that the occurrence of such phase transformation process imposes a time delay that is incompatible with the prompt response of the damage sensing function. This has led to a decision to locate the pre-load set point (αβ) at the point of plateau termination, making this the initial condition for the sensor function and thus assuring that phase transformation is completed before the instrument is exposed to the acceleration environment of flight. A plot of the stress-stain locus for either of the two identical wires is estimated for the damage sensor, in Figure 1b where, under effects of preload, a linear startup segment is seen, extending from the point of zero stress at the origin, to the point (α) at which the stress-induced phase transformation begins. Here the locus starts forming a curve that is seen to blend into a loading plateau which continues to point (αβ), where the wire has completed transformation to the martensite phase. This defines the state for both of the wires, in stress and strain, at the end of the "loading plateau". The point (α) marks the start of the stress induced phase transformation, begun here by the favorable orientation of particular crystals of the transformed martensite "variants" [3] as discussed in the following section. Transformation continues up to point (αβ) and ceases where the loading plateau ends. This occurs when the supply of transformable austenite is exhausted. The location of (αβ) defines the stress-strain conditions that preload settings have produced. The sensor is now prepared for use in sensing any further stress, imposed by the external acceleration environment. The dashed line locus, beyond point (αβ) , defines the path that a continuation of loading would produce in the α wire, under effects of acceleration. The plateau termination in strain, i.e."ε_{max}", is also an alloy property,

* "Superelastic" is a term used to describe the stress-strain locus displayed by a cycle of stress-induced phase transformation from austenite to martensite, when loading and then from martensite back to austenite on unloading. This plays a significant role in creating one form of shape memory, i.e., the form exploited in the sensor concept, i.e. austenite memory.

indicating that, at this strain and temperature transformation is complete. From here forward the elasticity of the material determines the stress-strain locus, as opposed to the stress-induced growth of martensite crystals, that had governed it on the plateau.

To this point it is seen that a linear segment of the stress-strain locus is produced, under the impetus of applied acceleration. As acceleration increases, the linear locus continues up to a maximum value produced at point (c), in a proportional response to the acceleration level. Note that this effect is only produced by acceleration that causes tension in the α wire. For oppositely directed acceleration, the β wire is in tension and therefore independently reacts to acceleration in that direction.

As load is reduced to zero from point (c), the stress-strain trajectory must follow a path that accommodates the yielding process the material has experienced. This effect is approximated by two downward straight-line segments in series. The first of these, segment (c-d), exists at increased slope, caused by islands of compressive back-stress, produced in reaction to localized tensile stresses, induced along the loading plateau. As noted by Mura [6], this is caused by the growth of martensite variants within an enclosing body of austenite which, in some cases, is locally loaded in tension to beyond its yield point by the effects of the level, all possible stress-induced phase interfering materials. During the unloading process, strain levels are initially recovered at a high rate due to the relaxation of back-stress* under reducing external load. The second segment, extending down to near zero stress from point (d), is initially dominated by the elastic modulus of the transformed material, a direct result of the completion of the stress-induced transformation. This converts to a horizontal unloading locus where reverse transformation occurs, terminating at ε_{resb}. For load reduction beginning at $\alpha\beta$, a similar locus is formed, terminating at ε_{resa}. The net effect is an increase in residual strain value by $\Delta\varepsilon_{res}$, as shown, due to the permanent deformation of austenite crystals, rendering them untransformable. This is a measurable effect, caused by the maximum values of experienced acceleration. The residual strain increment ($\Delta\varepsilon_{res}$) is thus a measure of stress applied to the material, thus providing a damage sensing capability.

* Back-stress is a form of compressive stress concentration that occurs in elastic structure in reaction to isolated islands of concentrated tensile stress [4], [6] and [7].

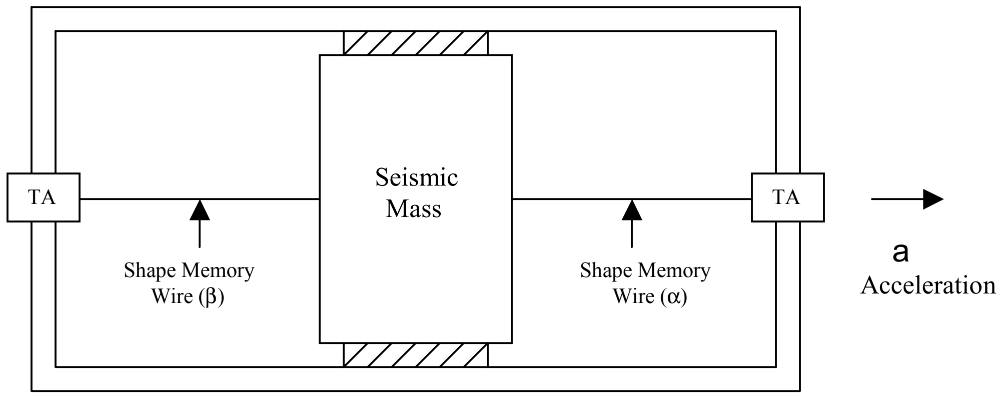

Figure 1a

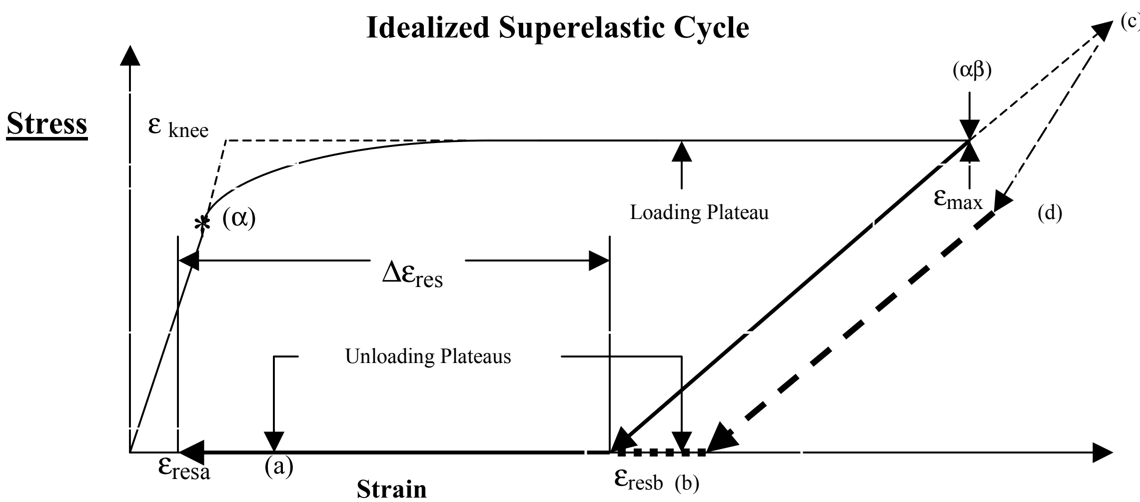

Fig 1b

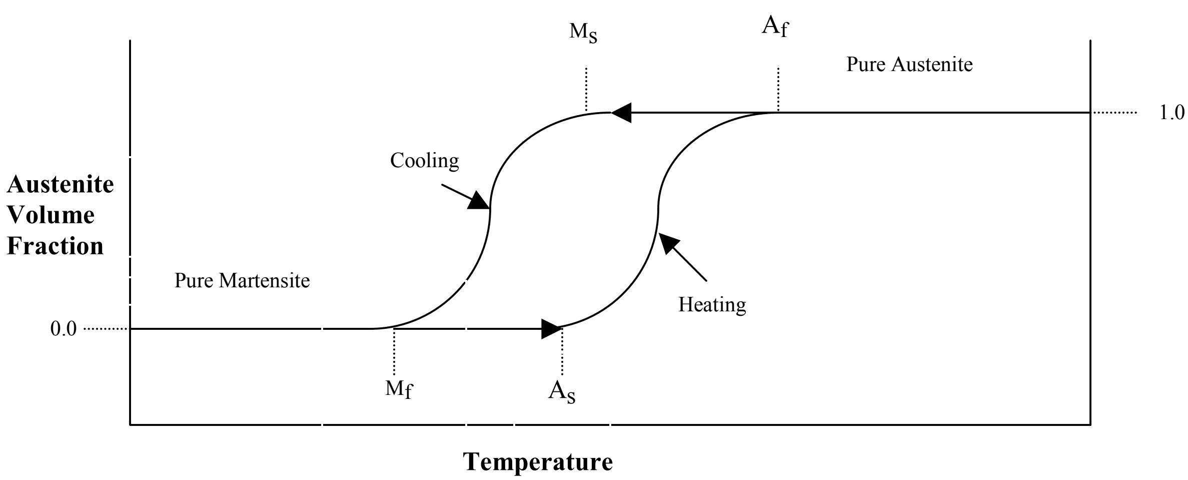

Fig 1c

Stress Induced and Thermally Induced Phase Transformations

Up to this point, a very general description of the sensor concept has been presented. Important issues of damage accumulation principles must still be addressed. Before beginning this, however, it is necessary to set the stage for such a discussion by describing certain salient aspects of phase transformation. This is addressed in the following.

The phase transformation discussed above is one of the two forms of transformation that give shape memory alloy its name. This type (i.e. stress-induced phase transformation) is caused by the application of tensile stress to shape memory material when it exists at a constant temperature that is within the temperature range at which the parent phase of the material exists. The parent phase is that crystalline form the material takes, when first cooled down from its molten state. This is referred to as "austenite". At temperatures below this range the material forms a finer grained phase called "martensite".

While the sensor concept is principally based upon stress induced phase transformation, a discussion of thermally induced transformation is necessary in order to understand the nature of the four transformation temperatures discussed herein. This follows.

On cooling from the austenite phase (usually a body centered cubic lattice) the material goes through a series of changes in crystal form until stabilizing in fine grained structure called "martensite"(usually having a face centered cubic lattice). The progression from austenite to martensite is illustrated by the cooling locus of Figure 1c. In this representation, progress from pure austenite to pure martensite is marked by three levels of transformation temperature: A_f (or "austenite-finish") above which a state of pure austenite exists), M_s (or "martensite-start") where martensite first begins to form on cooling, and M_f (for "martensite-finish") where the transformation to martensite is completed. It is noted that once a pure martensite phase is achieved by cooling, further removal of heat brings no further changes in the crystal lattice.

Upon application of heat, the material is returned to its parent phase, once more by traversing three transformation temperatures. Starting at M_f, the material is heated to A_s, at which temperature austenite structure first begins to form, and from there to A_f, where the transformation is complete (also shown on Figure 1c). By this process the material once again reverts to the typical parent crystal form of austenite. Note that all thermally induced transformations are performed with the material in a zero stress state, while in stress-induced transformation, the temperature is constant at a value equal to or greater than A_f but less than M_d* and stress is applied by external loading.

It is seen, in Figure 1b, that the loading plateau proceeds from (α) approaching the knee of the austenite start-up segment, (i.e. ε_{knee}) to termination (at ε_{max}). Throughout the length of this plateau, the stress-induced transformation is taking place within the enveloping parent phase, in the form of ellipsoidally shaped inclusions which nominally are aligned to the axis of external load. For a one-dimensional loading case, testing is performed on specimens of thin wire. In such cases it can be observed, through microscopic examination, that inclusions occur in approximate alignment to the axis of loading, parallel to the length of the wire. In a perception of the micro-mechanics of phase transformation, Mura [6] describes this as a formation of sub-domains of martensite inclusions that are formed within a primary domain of austenite where crystals of martensite, closely aligned to the axis of the wire, are initially formed. The sub-domain grows as stress increases and its austenitic enclosing structure deforms, in allowing for this growth. Thus transformation first occurs in bands of martensite that are most closely aligned to the applied external load. Depending on the yield strength of the austenite, some of this deformation is permanent, rendering that portion of austenite as untransformable. Thus a part of

* The M_d temperature is the maximum value at which stress-induced phase transformation can occur for a particular alloy. When at this value a shape memory material will exist in its parent phase, as pure austenite. Upon raising its stress level, an apparent loading plateau occurs at the yield strength of the material. This does not indicate an on-going phase transformation, but rather the creation of permanently deformedaustenite, which can no longer stress transformed to martensite.

the product phase is permanently deformed austenite, mixed with martensite.

Essential Properties of the Damage Sensor

The ability of the conceived damage sensor to do its job is dependent upon the existence of certain properties in its witness wires, permitting them the ability to achieve a state of yield under conditions of inertial loading that, for a proper design, goes beyond the strength limits of the structure upon which they are placed. The shape memory of the sensor depends upon this ability. The superelastic properties of the witness wires serve as a means to produce the conditions wherein a controlled yielding is produced, thereby ac-tivating the shape memory. In a superelastic cycle, yielding occurs in two forms:

(1) Starting from the austenite phase, a gradually increasing condition of yielding occurs as a result of the existence of "stress-induced martensite". This form of yielding is driven by a stress, produced in the austenite that surrounds a newly formed martensite crystal. This crystal exists in variants that form in near-alignment to the direction of applied stress. These crystals are of ellipsoidal shape that, as noted by Mura [6], force their austenitic enclosing structure into conforming shapes, accommodating their existence and growth. This process causes local stress concentrations, in some of the austenite, that exceed its yield strength. Thus local regions of yielding occur in directions of near conformance to the axis of applied stress. As previously noted, the permanent deformation sustained by the enclosing austenite structure, prevent that material's transformation, thereby producing a mixed product phase of newly formed martensite and deformed austenite. In its formation, the product phase shows a reduced dependence on applied stress, due to its stronger dependence upon crystal growth rather than elastic deformation under load. Thus a flat locus of stress and strain is formed, i.e. the so-called loading plateau. This process continues until all transformable austenite is converted to martensite.

(2) Upon the completion of the plateau formation, the stress-strain locus changes to a linear form, displaying a constant slope, consistent with the lower elastic modulus of the product phase. This linearity will persist until reaching the yield strength of the pro-duct phase. The inhomogeneity of the product phase, comprised of both martensite and deformed austenite, disrupts formation of a macroscopically uniform yielding domain. Thus a domain of distributed yielding is produced, as localized islands of concentrated stress are formed, due to the impingement of deformed austenite upon a now enlarged do-main of martensite crystals. The concentrations of impingement stress cause a yielding process to occur that is distributed across a relatively large range of strain, as is seen in the coming section on test results.

Experimental Test Results

In the following paragraphs test data is presented in plots of stress and strain, to provide a quantitative basis for the superelastic properties of the 5% Cu-Ni-Ti alloy. This is provided in discussions of individual plots, calling attention to features, which identify physical effects of importance to theory and the understanding of the material behavior.

In Figure 2, three superelastic cycles are presented at temperatures of 100, 110 and 125 degrees C. The objective of these plots is to illustrate the effects of the two forms of yielding, noted above, on the shape of the loading and unloading trajectories, the degree of superelasticity retained under increased load and, most important, the change in residual strain induced by increased loading beyond the loading plateau. These effects are important to the damage sensing conception and the test results provide data that support its validity. From this, it is seen that, at all three temperatures, significant shape memory is achieved. The maximum effect is observed at 110^0 C, at which a shape memory (i.e. $\Delta\varepsilon_{res}$) of 7 % is noted. At 100^0 C the shape memory is measured at 5.3 %, while at 125^0 C the shape memory is seen at 6 %. Conventional metering instruments may easily read all these values.

In figure 3a, below, the most significant observation is the essential equality of the stress levels of the loading plateaus at both 125 and 135^0 C. This implies that almost no stress-induced phase transformation is taking place along the plateaus at these temperatures. It is noted that at temperatures equal to or above the M_d value, this would occur. It is also noted that there are no obvious points of slope change on the 135^0 C locus while, for the 125^0 C case, such a point is barely visible on the loading plateau at a strain of approximately six percent. This is symptomatic of a completion of some small degree of a phase transformation. All of these observations suggest that the M_d temperature is either at 135^0 C or between that temperature and 125^0 C.

Other interesting aspects of Figures 2 and 3a are seen in the comparisons of residual strain, i.e. the shape memory, at the four temperatures. It is noted that, among all of the test results presented, four low-strain superelastic cycles have been run one at each temperature. All of these low-strain cycles show a perfect superelasticity, in that they re-turn to their origins at zero stress and strain. This indicates that no superelastic shape memory exists in these circumstances. This raises a question as to whether the shape memory effect depends upon both forms of yield or only upon type (2), i.e. that occurring beyond the loading plateaus. Figures 3b and 3c provide some insight into this issue.

From Figure 3b, it is seen that no shape memory exists, at either 100 or 110^0C, when strain does not exceed 9 %. At 125^0 C a shape memory of 6 % is seen. This would suggest that, for this alloy, yielding within the loading plateau produces no superelastic shape memory. From Figure 3c, for which three cycles of increasing maximum strain values are compared at 110^0 C, some shape memory (1.8 %) is noted when strain during loading has been raised to 13 %. For the case where a strain of 17 % is imposed, a shape memory of 7.5 % is noted. On the basis of this data it would seem that distributed yielding, produced at strain levels within the loading plateau, does not produce superelastic shape memory.

For our immediate purposes, it seems clear that for the 5% Cu-Ni-Ti alloy, sufficient shape memory has been demonstrated to support the damage sensor concept.

Test Results at 100 Degrees C for 5% Cu-Ni-Ti Alloy

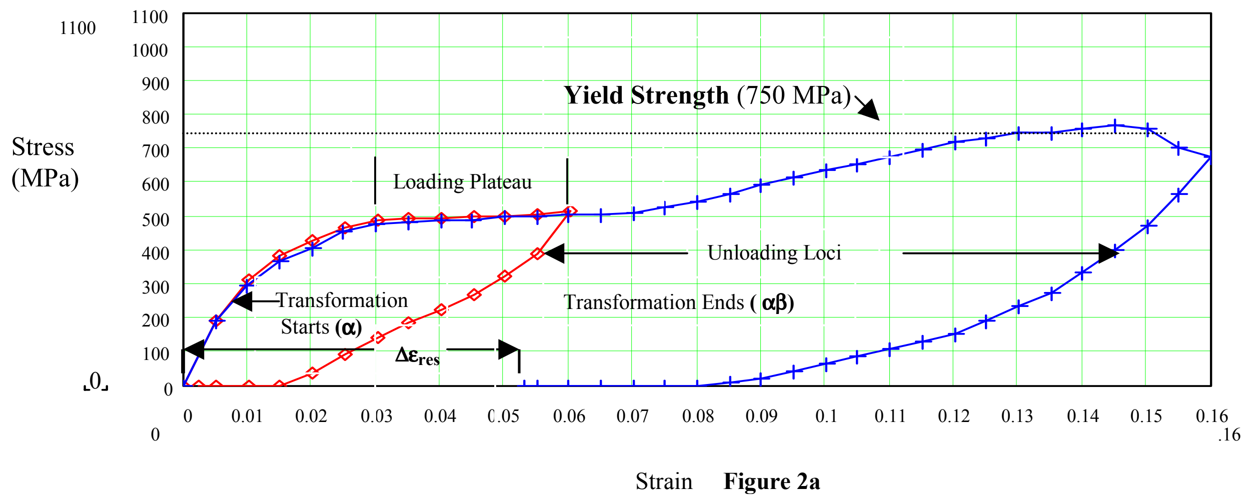

Figure 2a

Test Results at 110 Degrees C for 5% Cu-Ni-Ti Alloy

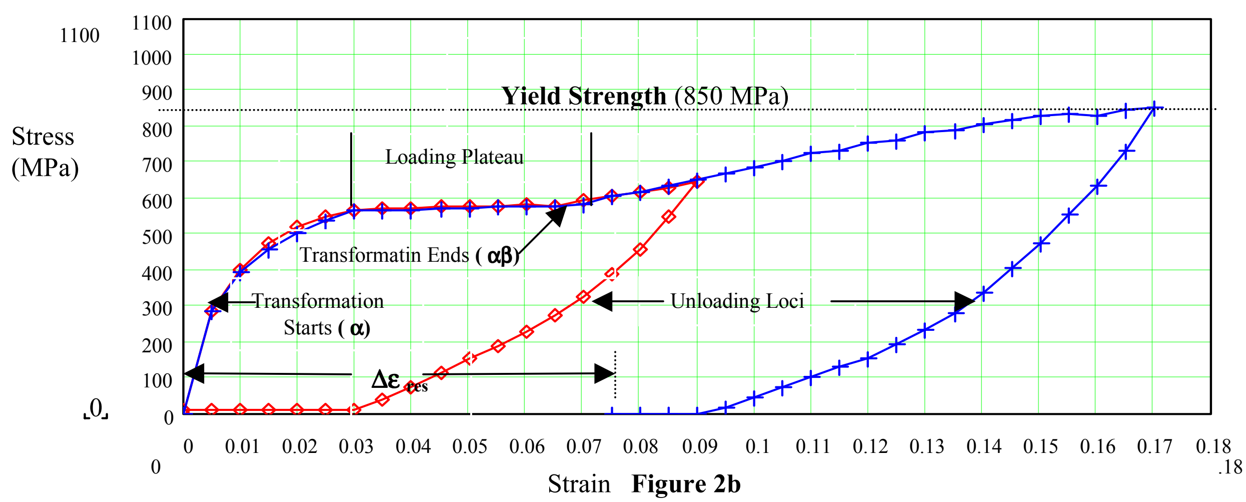

Figure 2b

Test Results at 125 Degrees C -5 % Cu-Ni-Ti Alloy

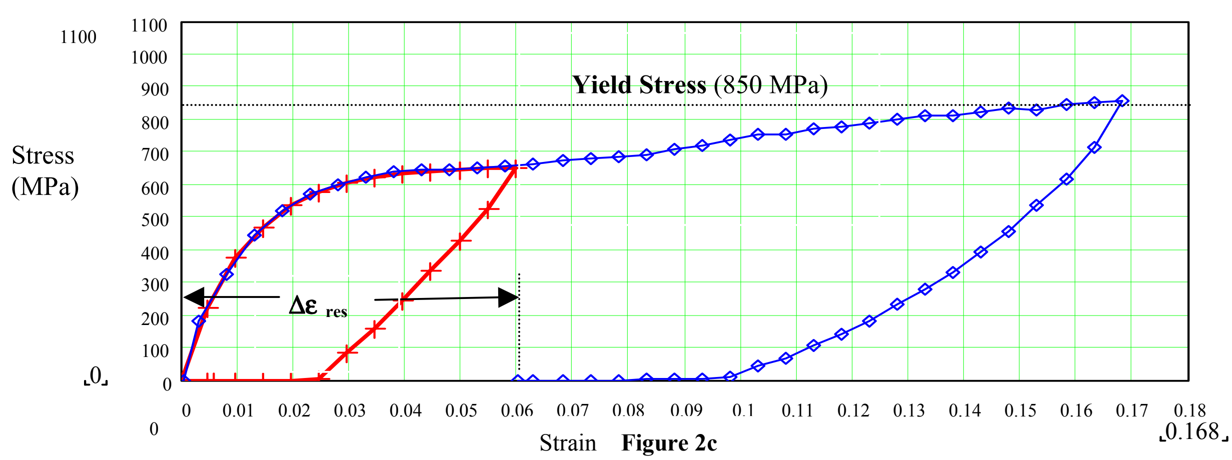

Figure 2c

Investigation into the M_d Value of 5% Cu-Ni-Ti Alloy
by comparison of Test Results at 125 and 135^0 C

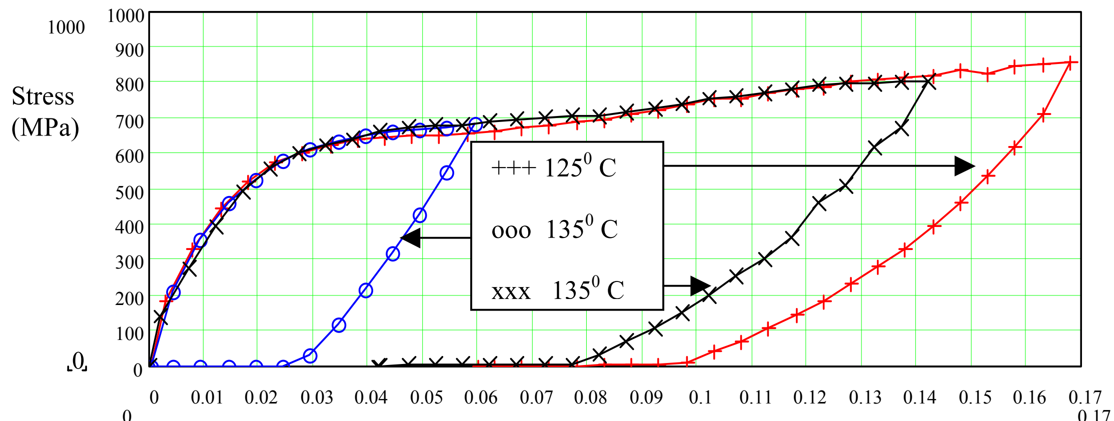

Figure 3a

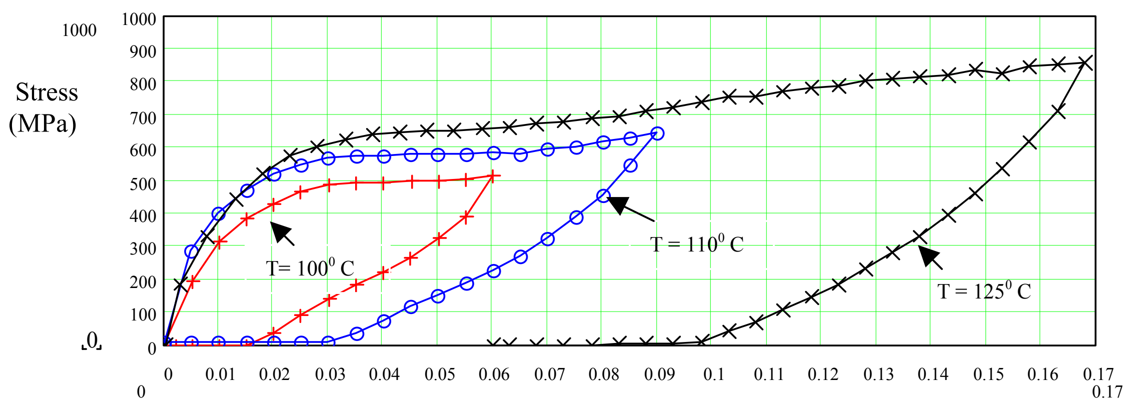

Figure 3b

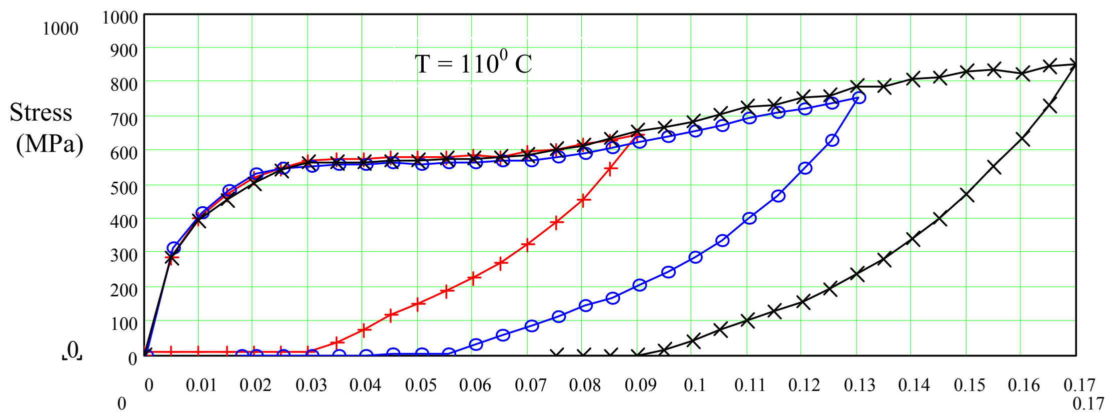

Figure 3c

Damage Sensing Described in a Hypothetical Experiment

In this section, a functional description of the damage sensor is presented, in context with its design features and the measured properties of the witness wires, to illustrate its perceived behavior and explain how the properties of these wires produce useful information through the change in residual strain that would be produced by exceeding a specific stress level, i.e. in this case the yield strength of the wires. The explanation is based upon the superelastic properties of the material, as presented in the test data plotted in Figures 3 and 4. This explanatory method is referred as a "hypothetical experiment" in which the properties of a stress-strain cycle, selected from test results, as reproduced in Figure 4a, are discussed.

The discussion is based upon analysis of a design conception for a damage sensor, displayed in Figure 4b, in formation of superelastic cycles for each of its two witness wires. The experiment is performed at 110^0 C, i.e. the temperature at which the largest increase in residual strain has been produced (see Figure 3b). The test cycles are hypothetically performed to demonstrate how the superelastic properties of an alloy may be exploited to accomplish damage sensing, based upon an imperfection in super- elasticity, i.e. a nonclosure of the hysteresis loops that occurs due to an episode of over-stress. The effect, as illustrated in Figure 4c, is traced through perceived stress-strain loci that would be produced in the conceived sensor design (per Figure 4b). This imperfection occurs in only certain shape memory alloys, i.e. those being abetted by the proximity of the testing temperature to the M_d temperature value. The imperfection in superelasticity has significant value in the sensor conception. In the following paragraphs the properties of shape memory alloys, of importance to the sensor concept, are applied to form semi-quantitative estimates, illustrating the potential value of the sensor conception.

The experiment begins by the loading of pure austenite that must exist at 110^0 C, as this exceeds the austenite finish temperature (A_f), shown as 76^0 C in Figure 4a. The loading proceeds in a linear stress-strain trajectory to point (α) where transformation be-gins. This shows a decreasing slope, indicative of an elastic modulus reduction due to the gradual growth of an initially small but gradually increasing amount of martensite variant which, as described by Lu and Weng among others [5], increases in quantity until point (b) is reached. At this location, remaining martensite formations are closely aligned to the axis of applied load and an almost horizontal trajectory of the stress and strain locus is produced. This continues until point $\alpha\beta$, i.e. at (c), where all transformable austenite is changed to martensite. At this location the plateau ends and the material, under further loading, displays a linear stress-strain locus.

The hypothetical experiment begins at the $\alpha\beta$ point of figure 4a and progresses on the assumption that if loading were to be continued beyond that point, by an acceleration event, the fully transformed material and untransformable austenite that exists in the pro- duct phase (at $\alpha\beta$), would produce a linearly rising locus segment, due to the elastic nature the material assumes when beyond the loading plateau. Such segments are visible in all the test data. If stress exceeds the yield strength of the material and then is unloaded, the unloading locus must follow a path (d-e) at a slope that exceeds that of the loading segment (c-d), due to the existence of the pockets of back-stress concentrations, discussed previously. Upon a partial release of external load the material assumes a lower slope, gradually finding equality with that of the (c-d) loading segment. The locus is seen to flatten at near-zero stress [point (f)], beginning its path toward the origin. This flattened segment is referred to as an "unloading plateau" which is the result of a "reverse phase transformation" from martensite back to austenite.

As can be seen in Figure 3c, this material, when loaded to a strain of 9 % at 110 degrees C, shows perfect superelasticity, a condition that changes significantly under an increasing load, reaching 7.5 % residual strain at a maximum applied strain of 17 %, as is seen in Figures 2b and 3a. This large imperfection in superelasticity (i.e. residual strain) serves as a permanent and measurable indicator that an over-stressed condition has been experienced. This is predictably caused by the exceeding of the material yield stress, estimated at 850 MPa, as shown in Figure 2b. The predictability arises from the expected permanent deformation, resulting from exceeding the yield stress. Thus, it is seen that the damage sensor concept is supported by a significant enlargement ($\Delta\varepsilon_{res}$) of residual strain. It is also noted that the 110^{0}C temperature is a suitable setting for temperature control.

The above cited test results indicate that a damage sensor can be developed that provides a permanent record of experienced maximum acceleration values, if the stress in its witness wires had exceeded the yield strength of the material's product phase. It is noted that stress levels, significantly higher than that value, would damage, and even fracture a witness wire. Once that occurs, all material memory is lost, but not all-physical evidence. If a wire is indeed fractured, one is justified in a conclusion that excessive stress had been experienced and thus a likely damaged component exists in a protected assembly that must be removed. Thus sensors with fractured wires would still have value.

Inspecting a Damage Sensor

In context with sensor objectives, the following two inspection methods are considered to offer practical, alternative inspection techniques:

(1) After a certain number of flights, that number being dependent upon statistical data analysis, a damage sensor is to be examined by direct measurement of the witness wires. This may be accomplished by its removal, from the system being protected and then disassembled permitting the witness wires to be inspected once they assume their natural dimension at room temperature conditions. The wires are then heated to repro-duce the sensor operating temperature and their lengths are measured, the results being recorded into a compilation of prior data, defining their original length, obtained before they had any exposure to inertial load. The difference between new and old readings pro-vides a measurement of the change in residual strain experienced due to the application environment to which the sensor had been exposed. If this is beyond a prescribed limit, the object of this protection, i.e. a critical component now established to be damaged, would be removed and replaced with a new component.

(2) Noting that a damaged sensor will always have a slack mass suspension, due to a permanently elongated witness wire, another way to inspect it is to develop an electro-mechanical device that can detect suspension slackness by applying and measuring the degree of tension adjustment required to snug-up each wire of a still-assembled sensor. Use of such a device provides advantages due to the time reduction to perform inspections and the quality of results derived from use of a non-invasive procedure.

It can be seen, in Figure 2b, that a change in residual strain after exposure to excessive acceleration, in which a yielding had been provoked, is seen to be 7.5 %. For a witness wire this might mean a preload induced increase of 0.075 inches is required, at a minimum, if one assumes a one-inch long witness wire is used. This is an estimate of the adjustment value required to remove the slack. If such a measurement is obtained, it must be concluded that the sensor had experienced (at least) the maximum permissible acceleration along one of its wires, indicating a need for preventive maintenance. This measurement can be accomplished by the development of a special tightening tool, to be used on the tension nuts, equipped with a multi-speed gearing mechanism and an angular transducer, capable of accurately measuring the necessary tightening changes to snug the wire and mass assembly up to its tightened state. The device must also be equipped with a load cell to detect wire assembly stiffening to inform the user that slack has been removed. If needed, a caging screw can be used to secure the inertial mass at the stiffened point that $\alpha\beta$ provides. This can be used in determining how much each witness wire is stretched.

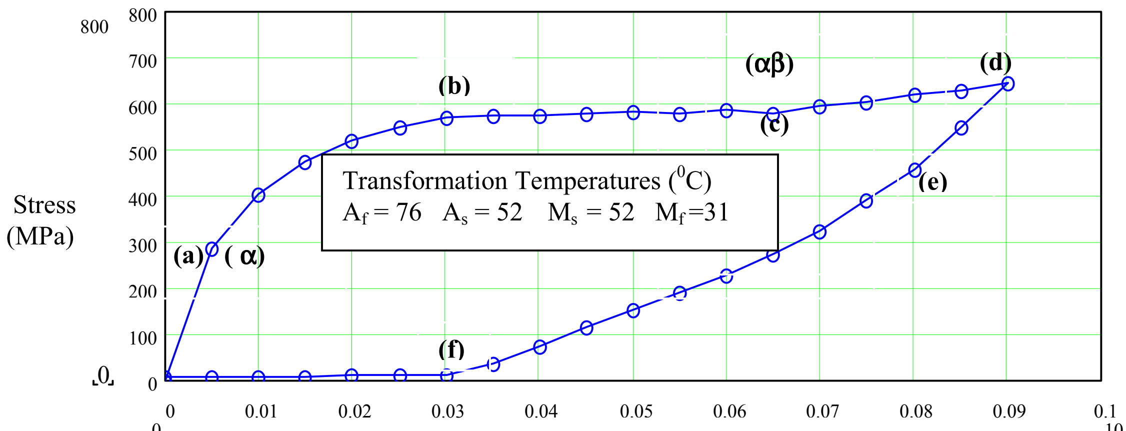

Figure 4a

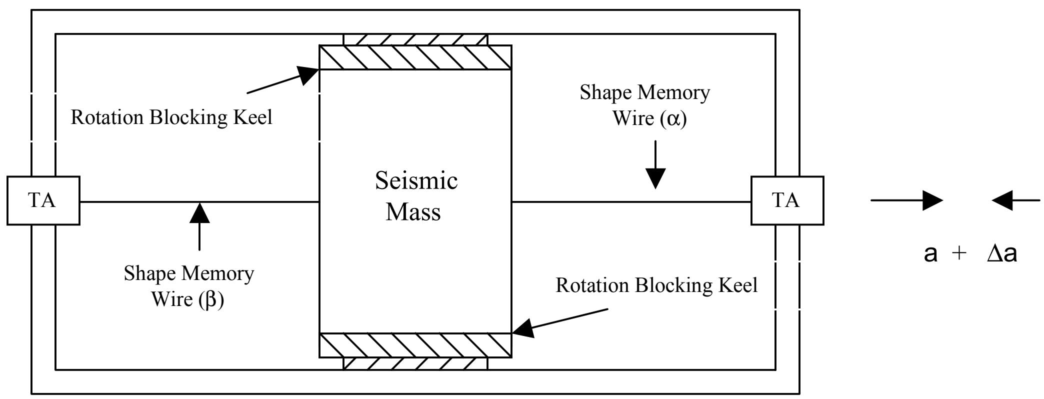

Figure 4b

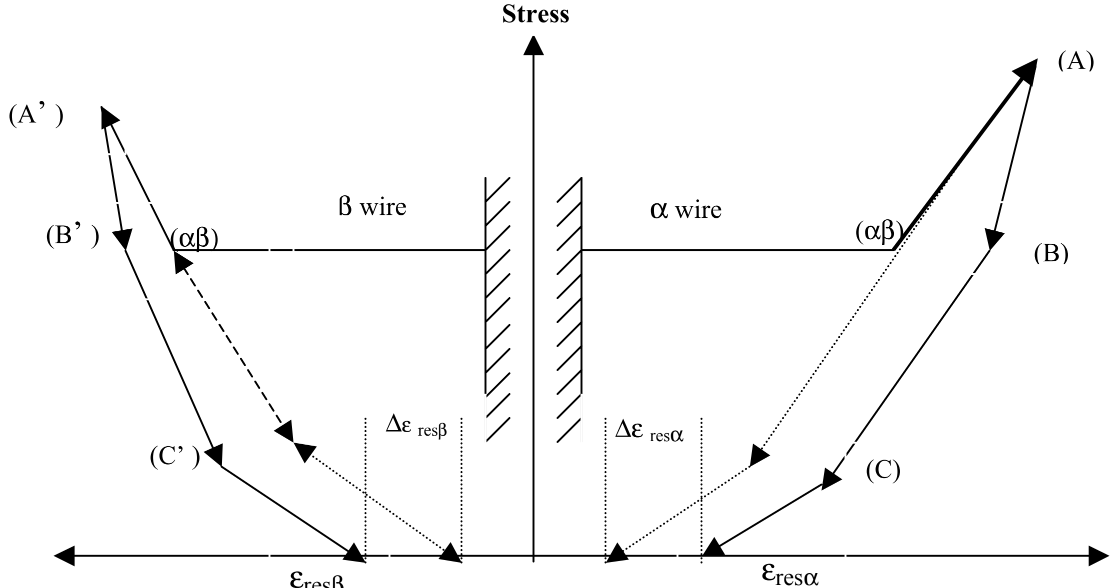

Figure 4c

Direction Sensing Capability

The prior discussions provide a general insight into how the shape memory alloy is expected to behave in a uni-directional sensor environment and how its effects are to be measured. The following considerations are presented to provide insight into the ability of the sensor to measure and discriminate between positive and negative accelerations. Note that segregation of the two directions is derived from the fact that only positive tensile force can influence the residual strain reading of a witness wire at the (αβ) point.

Considering the inertial effects on the mechanism shown in Figure 4b, if an acceleration vector (a) is initially applied, and then reduced by superimposing an equal valued acceleration vector (Δa), applied in the opposite direction, a simulation of inertial loading history would be accomplished. To achieve a simulation to the post-flight state, where the room temperature conditions would apply, a gradual reduction of preload stress is accomplished by the manual release of the preloading tension. The combination of these effects is judged to simulate a typical application environment. An estimation of a sensor's re-action to these circumstances is illustrated in Figure 4c. Results of this estimation are discussed in the following:

In the case for the α wire, as seen in Figure 4c, the acceleration vector (a) causes a linear stress-deformation increase from the αβ point up to point (A) which, by design, is beyond the yield stress of the product phase of the witness wires. Reducing stress from this point, by the superpositioning effect of Δa, would produce a reducing locus connecting (A) to (B). At this point the system, now under no inertial load, would be removed from its application and subjected to a further stress reduction, applied through a manual wire tension adjustment, to gradually reduce the preloading to a zero stress state.

Through these steps a reduction of the stress-strain loci from point (B) to (C) and thence to the zero condition of stress, would occur, thus simulating the conditions where the residual strain ($\varepsilon_{res\alpha}$) is produced. The disabling of temperature control would change these conditions, but the superelastic shape memory, invoked by reheating, would recover the needed data, allowing determination of inertially induced residual strain in the α wire.

The effect of the (a) vector on the β wire would seem to reduce its deformation on the loading plateau from the preload condition. However, this cannot occur along the plateau path. Instead, the preload stress effect will be reduced, along the linearly descending path seen in dashed lines for the β wire of Figure 4c. This will return to the loading plateau, i.e. point (αβ), as the α wire unloads to zero. The tendency to do this is represented by a double-headed arrow at the β side of the diagram. [Note that departure from the plateau path, illustrating the irreversibility of the plateau locus, is demonstrated in the work of Wolons, et al. [8]. Thus no permanent change in the length of the β wire will occur. If an additional acceleration event occurred subsequent to that measured by the α wire, but in a direction producing tension in the β wire, this effect would be measured by residual strain developed in the β wire and will have no effect on the α wire. This, of course, is the desired outcome. Thus, the acceleration component (Δa) does not produce any change in the α wire length, but only in that of the β wire, and conversely, the acceleration vector
(a) produces no change on the length of the β wire, but only on the α wire.

Feasibility Analysis

The following issues are identified as challenges to feasibility:

(a) Sensing Capability in a Practical Size - this is necessary to establish that the sensor concept is applicable for use within the assembly of electronic modules or within the various structures of an airframe body.

(b) Susceptibility to Environmental Damage -the very appearance of this wire suspended instrument raises questions about its ability to sustain the shock and vibration environments of transportation, handling, and flight.

(c) Cost – this must be shown to offer an advantage over the use of strain gages orother acceleration sensing instruments.

Sensing Capability in a Practical Size

The Damage Occurrence Sensor must provide indications that, in its prior use, it had witnessed acceleration levels considered excessive, in terms of a damage accumulation for the particular structure it is to protect. The sensor must be able to provide this indication to a pre-established accuracy and reliability over a specified range of acceleration.

To accomplish this, a design model is established to test possible design parameter alternatives that influence performance capabilities. The specifications, defining this capability, are presented as follows, along with discussions of its basis, for each separate requirement.

The size limits, defined in Figure 5a, identify the spatial constraints on instrument size, conceived as the dimensions of a rectangular prism that is to fit within a row of terminals of a typical printed circuit board. Numerical values for the terms defined here are indicated in the table of Figure 5b. In addition, the table includes material properties, and environmental limits for the sensor, along with the dimensions upon which they are based. Maximum acceleration values are defined as extending from 100 to 300 gs, the governing term for this being the seismic mass length (Lm), which can vary from 0.40 inches (at 300 gs) to 1.2 inches (for 100 gs). All other terms are constant, at the values shown. By using these numbers, the characteristics of the sensor are determined in the following analytical steps.

Sensor Space Envelope

$L_{enght} = 2 \times L_w + Lm + 2 \times t_w = 1.1$ to 1.9 inches

$W_{idth} = Dm + 2 \times b_h + 2 \times t_w = 0.80$ inches

$H_{ght} = W_{idtth} = 0.80$ inches

$G_{max} = 100$ to 300 gs

Figure 5a

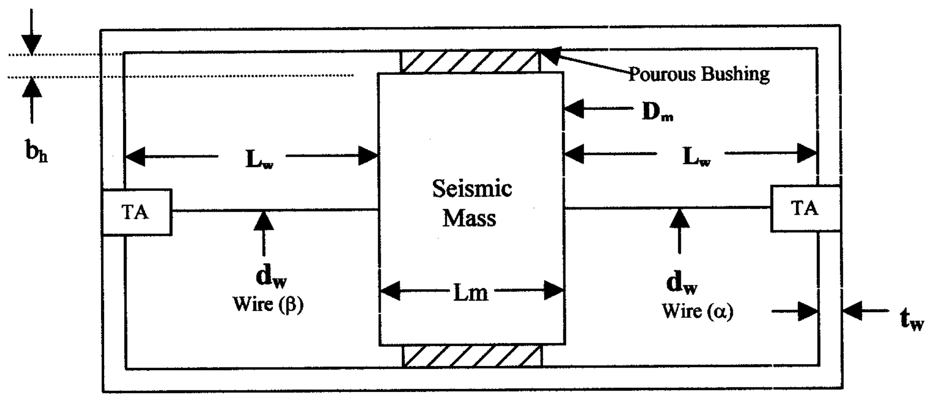

Parameter Values for the Design Model

Parameters	Symbols	Values
Alloy	Cu-Ni-Ti	5% Cu
Temperature	T	110^0 C
Effective Wire Length	L_W	0.30 in.
Wire Diameter	d_w	0.022 in.
Seismic Mass Length	Lm	0.400 to 1.200 in.
Seismic Mass Diameter	Dm	0. 600 in
Nominal Wall Thickness	$t_w = b_h$	0. 050 in
Bearing Thickness	b_h	0. 050 in
Alloy yield Strength	σ_y	123,278 psi (850 MPa) for the Product Phase at 110^0 C
Austenite Young's Modulus	E_{Aus}	8.9236 x10^6 psi (61,528 MPa)
Martensite Young's Modulus	E_{Mar}	2.2509 x10^6 psi (15520 MPa)
Seismic Mass Specific Weight	Sw_m	0.0610 lbs per in^3
Seismic Mass	M	0.006899 to 0.021038 lb sec^2/in
Specified Maximum Acceleration	G_{max}	100 to 300 gs

Figure 5 b

Quantification of Design Constraints

It is desired that the stress level, at points A and A′ of Figure 4c, be made equal to the yield strength of the witness wires. This is needed to assure a reliable memory of the acceleration event and still have some margin of measurement range to account for possible occurrences of stress that exceed expectations. The results of this is seen in figure 6b, in which an assumed fatal acceleration level produces stress slightly over the yield strength of the material for the specified wire diameter.

It is important to understand that a sensor designed for detection of a critical acceleration level of (say) 100 gs, cannot be used to protect a structure that fails at a lower level (say) e.g. 50 gs. Under these circumstances a different instrument scaling is necessary.

It is noted that a higher critical acceleration level produces a smaller instrument size.

Dynamic Analysis to Determine Transient Response of the Sensor

The maximum static stress level is produced by a reverse inertia force, assumed at 300 gs* in the following considerations, acting on a seismic mass of Mallory [9]. This is established under static load, however high acceleration levels do not often occur statically. Often they are caused by transient shock. Thus the design considerations. governing such an occurrence, must be addressed.

The following presents the salient points of a more detailed analysis. In this the basic differential equation, governing the motion of the seismic mass is derived and its solution is determined. This is extended to determine the witness wire stress under conditions of an abrupt application of 300 gs, applied along the sensing axis, as defined in the system concept shown in Figure 4b. In response to this input there will be overshoots in the responding deformations and stress. It is necessary to consider such conditions to determine system feasibility. To this end a spring-mass model having one degree of freedom (along the axis of the witness wire wires) is presented for analysis, in Figure 6a. The mass and the elasticity of such a structural system, determined from design calculations, based upon the information is presented in Figure 5b. In this case, damping is provided by the viscosity of a lubricant captured within the porous bushing. A derived differential equation of motion is given below. Note that its independent variable $\delta(t,T)$ is recognized as a function of temperature, as are the terms $\delta_p(T)$, D(T) and K(T). This equation is based on a free body diagram in which the instrument housing is considered to be part of a flight vehicle upon which a constant acceleration (a) is applied. Thus coordinate δ (t,T) defines motion of the seismic mass relative to the instrument housing. The analysis begins with derivation of the differential equation of motion, as follows. This is obtained through use of the Lagrange Formulation, for the system of Figure 5a, i.e.:

* The 300 gs was selected to provide an example of a level at which a minimum practical size of the instrument may be established. Such a level might be encountered in an anti-missile projectile, or in vortex hammer of an aircraft plowing through the wake of a large flight vehicle at low altitudes.

$$\frac{d}{dt}\left(\frac{\partial\Gamma}{\partial\left(\frac{d}{dt}\delta(t,T)\right)}\right)+\frac{\partial V}{\partial(\delta(t,T))}+\frac{\partial\left(R_{dp}\right)}{\partial\left(\frac{d}{dt}\delta(t,T)\right)} = Q$$

By use of this equation, components for inertial, damping and elastic force are defined.

$$\text{where : } \Gamma(t,T)= \frac{1}{2}\cdot M\cdot\left(\frac{d}{dt}\delta(t,T)\right)^2 \quad \text{defining Kinetic Energy}$$

and $\delta(t,T)$ is the coordinate for axial motion, as a function of time and temperature. Thus

$$F_{inertial}(t,T) = \frac{d}{dt}\left(\frac{\partial\Gamma}{\partial\left(\frac{d}{dt}\delta(t,T)\right)}\right) = \frac{d}{dt}\left[M\cdot\left(\frac{d}{dt}\delta(t,T)\right)\right] = M\cdot\frac{d^2}{dt^2}\delta(t,T)$$

$$R_{dp}(t,T) = \frac{D(T)}{2}\cdot\left(\frac{d}{dt}\delta(t,T)\right)^2 \quad \text{Rayleigh Dissipation Factor}$$

$$F_{damping}(t,T)= \frac{\partial\left(R_{dp}(T)\right)}{\partial\left(\frac{d}{dt}\delta(t,T)\right)} = D(T)\cdot\left(\frac{d}{dt}\delta(t,T)\right)$$

Note the α wire increases in tension while the β wire decreases, by virtue of the design.

$$V(t,T)= \left[\underbrace{\frac{K(T)}{2}\cdot\left(\delta(t,T)-\delta_p(T)\right)^2}_{\alpha\text{ wire term}}+\underbrace{\frac{K(T)}{2}\cdot\left[-\delta(t,T)+\delta_p(T)\right]^2}_{\beta\text{ wire term}}\right] \quad \text{Potential Energy}$$

$$F_{elastic}(t,T) = \frac{\partial V}{\partial(\delta(t,T))}$$

$$F_{elastic}(t,T)= \left[K(T)\cdot\left(\delta(t,T)+\delta_p(T)\right)+K(T)\cdot\left(-\delta(t,T)+\delta_p(T)\right)\cdot(-1)\right] = 2\cdot K(T)\cdot\left(\delta(t,T)-\delta_p(T)\right)$$

Synthesizing the above equation components according to the Lagrange Formulation and

noting that Q = M·a(t), we obtain:

$$M\cdot\frac{d^2}{dt^2}\delta(t,T)+D(T)\cdot\frac{d}{dt}\delta(t,T)+2\cdot K(T)\cdot\left(\delta(t)-\delta_p(T)\right) = M\cdot a(t) \qquad \text{…. (1)}$$

It is noted that, for isothermal conditions, this equation has constant coefficients. This is made possible by virtue of the chosen mechanization wherein the value of δ(0,T) is set to the termination point of the loading plateau. This prevents further transformation and thus prevents the time delays, associated with this process, from delaying the response of the system to further load. Thus when a transient acceleration, such as shock, is applied, the system response is immediate and the witness wires can respond to it and record its occurrence in a permanent length change. This also has the advantage of simplifying the analysis. Equation (1) is solved for the particular case of an acceleration step function at 300 gs, for which plots of mass motion [δ(t,T)] and witness wires stress [σ(t,T)] are presented against time in Figures 6a and 6b. The equations for these terms are given below:

$$\delta(t,T) = \frac{\left[G_{max}\cdot gc + \Omega_n^2(T)\cdot\delta_p(T)\right]}{\left[\Omega_n(T)^2\right]} - \frac{1}{\Omega_{nd}(T)}\cdot\left[\sqrt{\frac{(u(T)^2)}{(\Omega_n(T)^2)}}\right]\cdot e^{\frac{-D(T)}{2\cdot M}\cdot t}\cdot\cos\left(\Omega_{nd}(T)\cdot t + \psi(T)\right) \quad ...(2)$$

$$\sigma(t,T) = E_{trans}(T)\cdot\left(\frac{\delta(t,T)}{L_w} - \frac{\delta_p(T)}{L_w}\right) + \frac{S_{plat}(T)}{Cf} + \Delta\sigma(T) \quad \ldots (3)$$

Definitions of the terms in these two equations follow:

Regarding Equation (2):

$G_{max}\cdot gc$ = Input acceleration = Product of G_{max} and gc [local gravity value] (in/sec^2)

$\Omega_n(T)$ = Natural Frequency (rads/sec)

$\Omega_{nd}(T)$ = Damped Natural Frequency (rads/sec)

$$\Omega_n(T) = \sqrt{\frac{2\cdot K(T)}{M}} \quad .... (2a) \quad \text{and} \quad \Omega_{nd}(T) = \sqrt{\left[\frac{2\cdot K(T)}{M} - \left(\frac{D(T)}{2\cdot M}\right)^2\right]} \quad .... (2b)$$

$\delta_p(T) = \varepsilon_{max}(T)\cdot L_w$ which equals the mass displacement at the (αβ) point (inches)

D = Damping Coefficient (lb·sec per inch)

$$\psi(T) = -\operatorname{atan}\left(\frac{\frac{D(T)}{2\cdot M}}{\Omega_{nd}(T)}\right) \quad .... (2c)$$

Phase angle of the harmonic component of the transient response term

The equation for u(T) (as in the u(T) ^{2} factor of Equation 2) is derived as:

$$u(T) = \delta_p(T)\cdot\left[\left(\frac{D(T)}{2\cdot M}\right)^2 - \Omega_{nd}(T)^2\right] - \frac{D(T)^2}{4\cdot M^2}\cdot\delta_p(T) + \left(a + 2\cdot\frac{K(T)}{M}\cdot\delta_p(T)\right) \quad .... (2d)$$

Equation (1) is solved by use of Laplace transforms, thereby providing solutions which combine the transient response to the acceleration step function and the final value solution obtained for the particular integral.

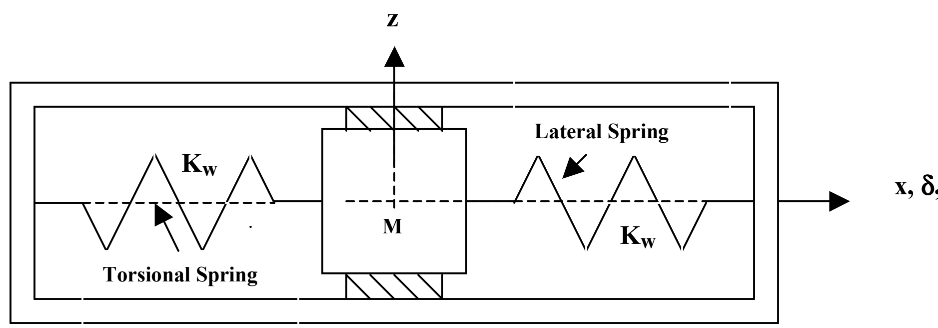

Figure 6a

The above diagram represents a single degree of freedom system which is used to model the damage sensor in its most vulnerable mode of motion. The motion, represented by δ, occurs along the designated x axis, allowing the mass M to translate in that direction. It is seen that the mass is restrained by two opposing springs which, due to the preload, will only experience tensile loads. The mass constrained against lateral motion by a cylindrical porous bushing that serves to lubricate the interfacial surfaces between the cylindrical mass and the bushing inner diameter. The lubricant is held in the pores of the bushing, by capillary forces, which permit it to leak out as the bearing absorbs heat, tending to keep its lubricating surfaces wet. Note that a torsional degree of freedom is suppressed by use of fin structure to prevent angular motion.

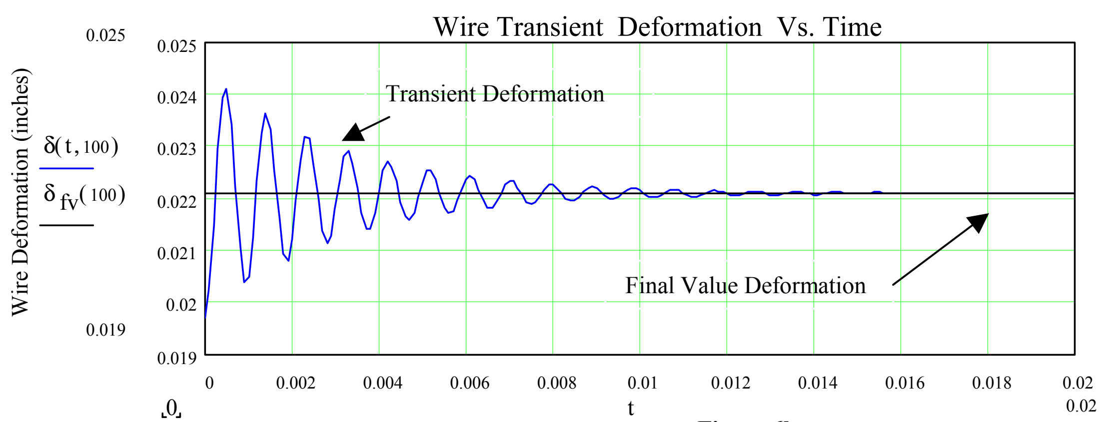

Figure 6b

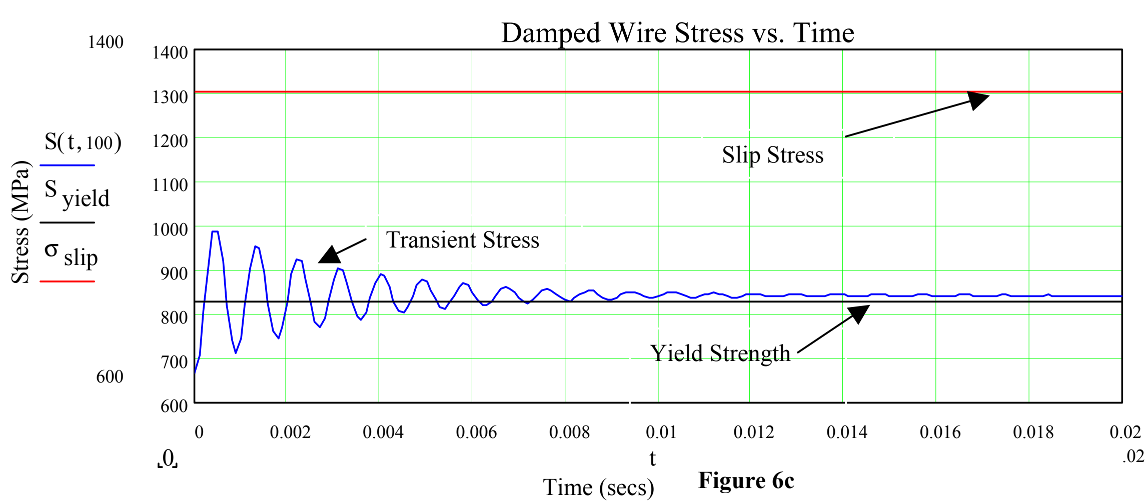

Figure 6c

Regarding Equation (3)

This equation is developed from physical considerations in which its value is seen to be an elastic effect proportional to the difference in strain between that produced by $\delta(t,T)$ and δ_p (T), which occurs at the plateau termination.

$E_{trans}(T)$ = Elastic Modulus (lbs per in^2): This is the value produced at the end of the loading plateau, where stress-induced phase transformation is complete and the alloy is a mixture of martensite and permanently deformed austenite.

$S_{plat}(T)$ = The stress of the loading plateau formation (psi): This is the stress level where stress-induced phase transformation begins. This parameter is proportional to the quantity ($T - M_s$). [Note Cf is the conversion factor from MPa to psi.]

$\Delta\sigma(T)$ = The stress increment between plateau formation and plateau termination: This effect is largely proportional to the latent heat of phase transformation (a constant for the alloy). It is also affected by a temperature gradient along the witness wires. Its value is obtained from the test data plots of Figure 2a and 2b.

The analysis and plots of damped wire deformation, in figure 6b, and damped wire stress, in 6c, provide a basis for the following discussions and conclusions:

Issues of Environmental Damage to the Sensor

(A) Low cycle fatigue due to multiple exposures to sudden acceleration events.

Nominal step accelerations in the range of 300 gs or less are expected to produce maximum dynamic stress values of less than 15,000 psi. As the yield stress of the material is over 120,000 psi, the dynamic stress is less than 13 % of the yield stress, a condition that, from stress-based fatigue analysis considerations, would generally eliminate low cycle fatigue failure. However, in view of the local stress concentrations at work in the transformation process, one must proceed with caution, in this regard. These circumstances suggest that a strain-based assessment of the low cycle fatigue probability is in order. This equires a detailed design analysis, which is to be presented in a second paper where such detail is established. It is noted that while the results of this work may alter the design details, presented herein, it is not expected to challenge the feasibility of the concept, although it may influence the scaling, to some extent. This observation is based upon the fact that the wire diameter and the maximum permissible acceleration level should be optimized for each particular flight vehicle being used. Thus they can also be optimized for low cycle fatigue effects, should that prove to be necessary.

(B) High Cycle Fatigue Induced by Transient Stress

The possible accumulation of high stress reversals due to transient response of the system, in reaction to the external acceleration events, is seen in Figure 6c. In this circumstance a reversing stress component is predicted having zero-to-peak maximum amplitude of about 16,000 psi (110.32 MPa), which diminishes to zero over approximately fifteen cycles. A sustained application of this maximum vibratory component, applied at an average stress equal to the yield point of the material, would suggest a poor fatigue life of several hundred cycles. This would, at least, be doubled by the decaying amplitude effect, shown in that plot, suggesting a minimum life in the realm of a thousand incidents of this transient stress function. The probability that such an accumulation of stress reversals, of this nature, is very low because a sensor would have been removed and replaced, in the preventive maintenance process, after the first such exposure to a yielding condition. For this reason, fatigue due to accumulation of transient stress cycles is not considered a threat.

The accumulation of stress reversals may also occur due to resonance of the sensor wires excited, by the aircraft engines. This could cause fatigue, depending upon the location of the sensor relative to the engine itself. In this case the vibration level would have to be severe enough to produce a wire fatigue failure and such severity would also be a problem to other aircraft components. Thus a fatigue failure, induced in a sensor, is consistent with its basic function, to warn of an extraordinary and potentially dangerous engine vibration condition that needs corrective action. While a wire fatigue failure destroys the data record provided by a sensor, its recognition as fatigue provides a warning that improper conditions exist. This is consistent and in keeping with the purpose of the damage sensor and part of its function.

(C) Destructive modes of resonant vibration

Such modes can be caused by the existence of degrees of freedom that are unnecessary for the basic function of the sensor. It was recognized at the beginning of the design conception that permitting angular motion to occur about the x axis of Figure 6a would enable a low frequency mode of vibration that could be in a state of constant first order resonance with aircraft engine rotor rotation rates. The existence of such an effect has been verified by calculation and it was concluded that this unnecessary degree of freedom must be eliminated. This is accomplished by a pair of rotation blocking keels on a common diameter of the seismic mass. The keels will limit the angular motion about the wire sensing axes, without interfering with motion along that axis. The concept of the keels (not included in the schematic drawings of the sensor) involves the use of fins attached internally to the instrument housing and extending radially inward from the porous bushing, to enter shallow grooves in the seismic mass at diametrically opposed locations, thereby serving to essentially block out rotation of the torsional spring (effected by the two witness wires).

(D) Cost Considerations

The sensor conception was developed to offer a low cost device for an application that requires it to be expendable. The basic design concept, shown schematically in this paper, is strongly influenced by the idea that a simple construction, involving few parts, is essential for this component. Furthermore, because the need for this sensor extends to all applications in which shock effects degrade the usefulness of much more expensive products, sensor manufacturing can develop large economies of scale. It is perceived that many thousands of sensors will be required, for use around the world, in commercial aviation, but there is no reason to limit applications to this market. A large military market is also perceived, in which the sensor could serve both aviation and ground force vehicles, such as armored tanks and other forms of mobile artillery. It is expected that a successful design will command an annual production volume in the hundreds of thousands of units. In such circumstances the economies of scale would permit low selling prices, their values to be determined in the detailed design of the sensor.

Conclusions

It is our conviction that the Passive Damage Occurrence Sensor with its unique application of shape memory material will benefit society in many ways.

- First, it should reduce the number of aircraft accidents and the loss of life inboth commercial and military applications.
- It permits the finding of damage, through inspection, that presently is hidden to the eye making that inspection more effective.
- It will reduce the cost of insurance.
- Its application by the military will reduce the immense cost of supplying and maintaining combat and transportation vehicles.
- The added safety in flight should increase revenue for passenger service and reduce the transportation costs of sending manufactured products to market.
- The sensor concept is feasible and can be brought into being through further development.
- The basic physical properties that are exploited, in the passive damage sensor conception are unique and dependent upon the properties of a shape memory alloy for the following reasons:

  1) The irreversible phase transformation that is set into the witness wires, by pre-loading them to the transformation completion point of the damage sensor, together with the nature of the sensor design, prevents lost memory in a tension wire due to reversal of acceleration direction. This is not possible with any other type of material or design.

  2) The property of shape memory of the witness wires to be used in the damage sensor allows maintenance of a non-erasable record of loading history. The non-erasability prevents the loss of knowledge of an excessive loading episode. This is only accomplished with

shape memory alloys having superelastic properties. Should a ductile non-superelastic material be used for the sensor witness wires, for example the ASTM A514 steel, unloading from stress levels around the yield point would produce residual strain values of less than 0.3% when loaded to724 MPa, as opposed to values greater than 7 % for the superelastic material when loaded to 850MPa. Large values of memory for the ductile steel would require loading beyond the peaking value of the engineering stress-strain loci, resulting in an unstable strain increase to fracture, thereby losing memory of a high stress episode.

3) The micromechanics of stress-induced phase transformation permits isolated islands of internal stress concentrations to be formed, causing localized yielding to occur at levels of applied stress below the value at which a total yielding is produced in the material. As applied stress increases, the islands are brought up to and beyond yield strength level. Due to the local nature of the stress, the material retains a positive slope in its stress-strain locus throughout its range of use and thus occurrence of unstable load resistance is precluded.

- It is concluded that the concept should be developed into a product.

Acknowledgements

Testing was performed at Memry Inc. in Bethel CT to obtain the benefits of the test equipment and knowledge that resides there.

References

1. AirSafe.com: A web based news service for the Civil Aviation industry.

2. Air Wise News 10/15/2003: A news service for Civil Aviation.

3. Brinson, L. C.: One-Dimensional Constitutive Behavior of Shape Memory Alloys: Thermo-mechanical Derivation with Non-Constant Material Functions and Redefined Martensite Internal Variable", J. of Intelligent Material Systems and Structures, Vol. 4 – April 1993

4. Jastrzebski, Z.: "Nature and Properties of Engineering Materials". See Bauschinger Effect page 212 published by John Wiley & Sons, Inc.

5. Lu, Z. K. and G. J. Weng: "Martensitic Transformation and Stress-Strain Relations of Shape Memory Alloys", J. of Phys. Solids, Vol 45, No. 11, 12, 1997

6. Mura, T.: "Micromechanics and Defects in Solids" 2nd Revised Ed., Martinus Nijhoff Publishers

7. Timoshenko, S.: "Strength of Materials- Part II *Advanced Theory and Problems*" 2nd Edition, 13th printing. See Residual Stress on Page 417. Published by D. Van Nostrand and Company Inc.

8. Wolons, D., Gandhi, F. and Malovrh, B.: "Experimental Investigation of the Pseudoelastic Hysteresis Damping Characteristics of Shape memory Alloy wires", J. of Intelligent Material Systems and Structures, Vol. 9 – February 1998.

9. www.mallory.com